On Anisotropic Geometric Diffusion in 3D Image Processing and Image Sequence Analysis

Karol Mikula[1] Tobias Preußer[2] Martin Rumpf[2] Fiorella Sgallari[3]

Abstract

A morphological multiscale method in 3D image and 3D image sequence processing is discussed which identifies edges on level sets and the motion of features in time. Based on these indicator evaluation the image data is processed applying nonlinear diffusion and the theory of geometric evolution problems. The aim is to smooth level sets of a 3D image while preserving geometric features such as edges and corners on the level sets and to simultaneously respect the motion and acceleration of object in time. An anisotropic curvature evolution is considered in space. Whereas, in case of an image sequence a weak coupling of these separate curvature evolutions problems is incorporated in the time direction of the image sequence. The time of the actual evolution problem serves as the multiscale parameter. The spatial diffusion tensor depends on a regularized shape operator of the evolving level sets and the evolution speed is weighted according to an approximation of the apparent acceleration of objects. As one suitable regularization tool local L^2–projection onto polynomials is considered. A spatial finite element discretization on hexahedral meshes, a semi-implicit, regularized backward Euler discretization in time, and an explicit coupling of subsequent images in case of image sequences are the building blocks of the algorithm. Different applications underline the efficiency of the presented image processing tool.

I. Introduction

Processing three dimensional images and image sequences is a task of growing interest in various applications. Especially in medical imaging different image generation hardware such as CT or MRI devices, and more recently also 3D ultrasound devices deliver large image data at high resolution for further post processing. Based on that data anomalies can be analyzed and the progress of deseases can be studied. Furthermore, physical experiments can be recorded via MRI or other 3D measurement devices. Thus comparisons with 3D simulations became possible. Frequently the resulting images and image sequences are characterized by a rather unsatisfying signal to noise ratio, which leads to serious difficulties in the further post processing. Especially in 3D many features are hidden and the essential structure or the involved motions and developments are hard to catch visually. Frequently, one is interested in the extraction of certain level surfaces from the data, which bound volumes or separate regions of interest. Often the actual intensity value is of minor importance and dependent on the modality in the image generation process. Methods which behave invariant under transformations of the intensity or gray scale are called morphological. They only effect the morphology of the image, which coincides with the geometry of the level sets. The aim of this paper is to combine recent results on anisotropic geometric diffusion for the denoising of 3D images and a smoothing method for 3D image sequences which takes into account feature motion and acceleration. The peculiarity of the method is, that it is able to preserve edges and corners on level sets while still allowing tangential smoothing along the edges. Furthermore, a suitable acceleration quantity — the apparent acceleration — is used to modulate the speed of propagation.

The core of the method is an evolution driven by *anisotropic geometric diffusion* of level surfaces. In case of image sequences the diffusion processes are coupled on different frames of the sequence in time and then simultaneously applied to every frame. Thus, an anisotropic diffusion tensor depending on a presmoothed shape operator and thus on presmoothed principal curvatures and principal directions of curvature, is sensitive to the identification of the important surface features. Furthermore, the speed of diffusion is modulated based on the measured motion of level sets in image sequences. In the identification of curvature and motion quantities, a build-in regularization and projection on prototype shapes turns out to be essential to make the proposed method robust and mathematically well-posed.

The paper is organized as follows. First, in Section II we discuss some background work on image and image sequence processing. Section III briefly introduces the anisotropic geometric diffusion method on still images and in Section IV we discuss the generalization to image sequences via a suitable coupling of the diffusion problems on different frames of the sequence. Afterwards, in Section V we sketch how to extract the required curvature and motion quantities and in Section VI we present the actual discretization with finite elements.

II. Review of related work

Let us consider a noisy image given by an intensity map $\phi_0 : \Omega \to \mathbb{R}; x \mapsto \phi_0(x)$ on some image domain $\Omega \subset \mathbb{R}^3$ or a continuous image sequence $\phi_0 : [0,T] \times \Omega \to \mathbb{R}; (s,x) \mapsto \phi_0(s,x)$. Scale space methods define an evolution operator $E(t)$ which acts on the initial data ϕ_0 and delivers a family of representations $\{E(t)\phi_0\}_{t\geq 0}$ on successively coarser scales. Here, the time parameter t acts as a scale parameter, leading form a fine, but noisy representation for time $t = 0$ to successively smoother and coarser representation for increasing time parameter t. To avoid any confusion we will always use t for the time scale of the smoothing evolution and s for the sequence parameter, which represents time in the image sequence data base. One of the first

[1]Department of Mathematics, Slovak University of Technology, Bratislava, Slovakia (mikula@vox.svf.stuba.sk)
[2]Faculty for Mathematics, University of Duisburg, Duisburg, Germany ([preusser, rumpf]@math.uni-duisburg.de)
[3]Department of Mathematics and CIRAM, University of Bologna, Bologna, Italy (sgallari@dm.unibo.it)

successful methods along this concept was presented by Perona and Malik [24]. For a given initial image ϕ_0 they considered the evolution problem

$$\partial_t \phi - \operatorname{div}(G(\|\nabla\phi\|)\nabla\phi) = 0$$

For increasing time t - the scale parameter - the original image at the initial time is successfully smoothed and image patterns are coarsened. Simultaneously edges - indicated by steep image gradients - are enhanced if one chooses a diffusion coefficient $G(.)$ which suppresses diffusion in areas of high gradients. A suitable choice is $G(\alpha) = \left(1 + \frac{\alpha^2}{\lambda^2}\right)^{-1}$ for a positive constant λ. Catté et al. [6] proposed a regularization method where the diffusion coefficient is no longer evaluated on the exact intensity gradient. Instead they suggested to consider the gradient evaluation on a prefiltered image, i.e., they consider the equation

$$\partial_t \phi - \operatorname{div}(G(\|\nabla\phi_\sigma\|)\nabla\phi) = 0$$

where $\phi_\sigma = K_\sigma * \phi$ with a suitable local convolution kernel K_σ of width σ. Compared to the original Perona–Malik method this model turns out to be well-posed and edges are still retained. Indead, the prefiltering avoids the detection and pronouncing of artificial edges, which are due to the initial noise.

Weickert [34] improved this method taking into account anisotropic diffusion, where the Perona–Malik type diffusion is concentrated in one direction, for instance the direction perpendicular to the level set or feature direction. This leads to an additional tangential smoothing on level sets and enables to amplify intensity correlations along lines or on level sets. The geometry of this evolution problem especially influences our investigations on anisotropic diffusion. In the axiomatic work by Alvarez et al. [1] general nonlinear evolution problems based on the scale space idea where derived from a set of axioms. Especially including the axiom of gray value invariance they end up with a curvature evolution model, i. e.

$$\partial_t \phi - \|\nabla\phi\| \left(t \operatorname{div}\left(\frac{\nabla\phi}{\|\nabla\phi\|}\right)\right)^{\frac{1}{3}} = 0\,.$$

Curvature motions has been studied for a long time in geometry and in physics, where interfaces are driven by surface tension. In dimensions higher than two, singularities may occur in the evolution. Existence of generalized viscosity solutions has been proved by Evans and Spruck [13]. Anisotropic curvature flow has been studied for instance by Bellettini and Paolini [5]. In case of planar curves Kačur and Mikula [19] considered an evolution equation for the curvature, from which one can recover the shape of the curves. Concerning the application this is closely related to the preferability of certain interface orientations in the crystalline structure of material (cf. [3], [31]). Starting with the above mentioned axiomatic results curvature motion proved to be a successful ingredient in segmentation and image enhancement methods, e. g. compare Pauwels et al. [23]. Sapiro [28] proposed a modification of Mean-Curvature-Motion (MCM) considering a diffusion coefficient which depends on the image gradient.

In [7] a parametric anisotropic curvature motion was applied to the smoothing of noisy triangulated surfaces. It preserves edges on the surfaces and incorporates diffusion solely along the edge and not perpendicular to it. In [26] a corresponding level set formulation has been discussed and compared to the parametric model. This method will be presented in detail below and enter our image sequence smoothing scheme via the involved spatial operator.

Motion detection in image sequences is already a classical research area in computer vision. Various approaches have been presented to extract object velocities from movie data and the motion or deformation of objects therein. Either one asks for a deformation controlled by elastic stresses where the elastic properties may depend on knowledge about the material or one considers flow fields which give rise for the deformation. For details we refer to [32], [18], [8]. Alternatively, optical flow techniques can be implied, which are based on suitable regularization of the inverse problem to identify the deformation [22], [11], [2], [27], [34]. An axiomatic scale space theory for continuous image sequences has been developed by Guichard [14].

Mikula et al. [21] presented an extension of the original Perona–Malik approach to image sequences via a modulation of the propagation speed depending on a measured acceleration quantity. The speed modulation presented here will be based on these results. In their model they consider a quantity introduced by Guichard [15] which assumes that points preserve their intensity along the smooth (*lambertian*) motion trajectories, i.e. they proposed a finite volume scheme for the scale space model for image sequences $\phi : \mathbb{R}^+ \times [0,T] \times \Omega \to [0,1]$

$$\partial_t \phi - \operatorname{clt}(\phi_\sigma)\operatorname{div}(G(\|\nabla\phi_\sigma\|)\nabla\phi) = 0$$

where the index σ indicates a usual regularization. The so called *curvature of lambertian trajectories* $\operatorname{clt}(\phi)$ at time s for scale t is defined by

$$\begin{aligned}\operatorname{clt}(\phi)(t,s,x) := \lim_{\Delta s \to 0} \min_{w_1,w_2 \in M} \frac{1}{(\Delta s)^2}\Big(& | < \nabla\phi(t,s,x), w_1 - w_2 > | \\ & + |\phi(t,s-\Delta s, x - w_1) - \phi(t,s,x)| \\ & + |\phi(t,s-\Delta s, x + w_2) - \phi(t,s,x)|\Big),\end{aligned}$$

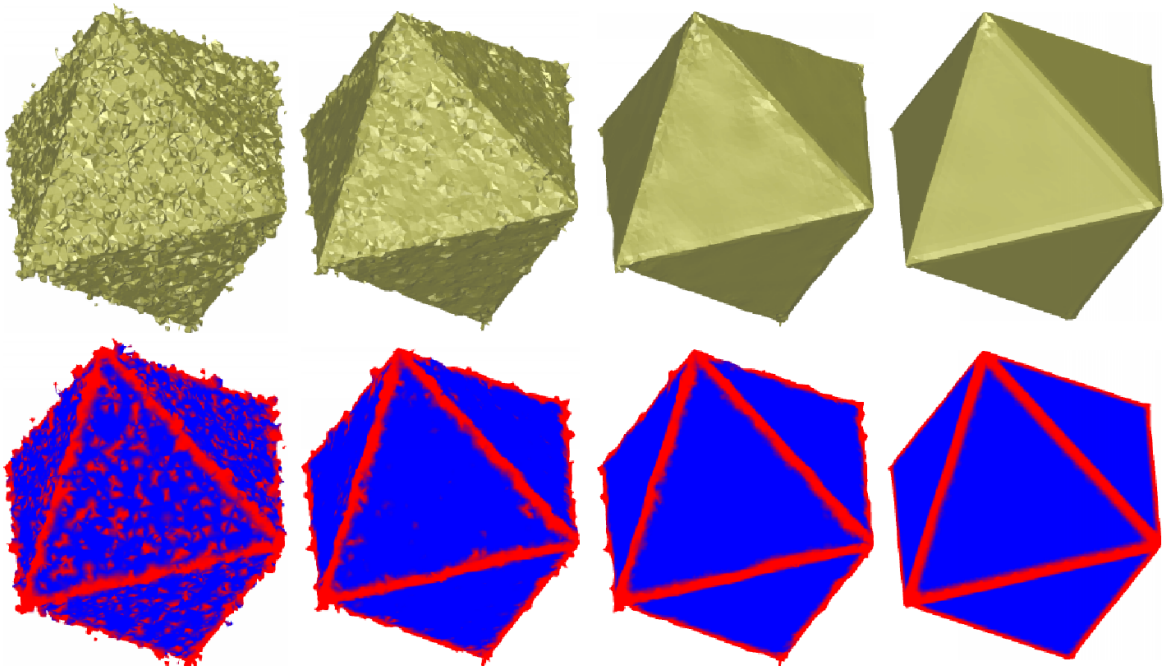

Fig. 1. *As a test case for the anisotrpic geometric diffusion for still images we consider the function $\phi(x) = |x_1| + |x_2| + |x_3|$ whose level sets are octahedrons. This function was perturbed and then taken as initial data for the anisotropic geometric diffusion method for single images. From left to right an original perturbed level set and the corresponding first, second, and fifth time step of its evolution on a 64^3 grid are depicted. In the bottom row we visualize the dominant curvature on the level sets from the left column. A color ramp from blue to red indicates the dominant curvature value.*

where M is a small ball around x. It measures the coherence of the moving structures in time. The first part of the $\mathrm{clt}(\phi)$ definition actually measures the so called *apparent acceleration* and the second and third term evaluate gray value coherences. In the implementation one confines with Δs being the time offset between two frames of the given discrete image sequence and considers M as a discrete ball of pixels around x.

Concerning the general numerical implementation of PDE methods in image processing among others Weickert proposed finite difference schemes [34] and Kačur and Mikula [16] suggested a semi-implicit finite element implementation for the isotropic model by Catté et al.[6]. Adaptive finite element methods in image processing are discussed by Bänsch and Mikula [4], Schnörr [30] and in [25]. Kimmel [17] generalizes scale space methodology to textures on surfaces, considering the appropriate intrinsic differential operators. A finite volume implementation has been studied by Mikula and Ramarosy [20].

The numerical approximation of curvature motion in level set form has recently been investigated by Deckelnick and Dziuk [9]. They have analyzed a corresponding fully discrete finite element method and proved convergence toward viscosity solutions.

III. Anisotropic geometric diffusion on still images

At first, we confine to the processing of still images. Thus, we consider a noisy initial image $\phi_0 : \Omega \to \mathbb{R}; x \mapsto \phi_0(x)$ with $\Omega \subset \mathbb{R}^3$ and ask for a scale of images $\{\phi(t,\cdot) \,|\, t \geq 0\}$ with $\phi(0,\cdot) = \phi_0$. Throughout this paper Ω will always be the unit cube $[0,1]^3$. We will define a level set formulation for a generalized anisotropic curvature motion of the isosurfaces.

Here, as long as we derive the model we assume $\phi(\cdot,\cdot)$ to be sufficiently smooth and $\nabla\phi(t,x) \neq 0$ for all $(t,x) \in \mathbb{R}_0^+ \times \Omega$. Indeed, due to the implicit function theorem the corresponding level sets are actually smooth surfaces.

To keep our method invariant under gray scale transformations we confine to curvature quantities as the driving forces for the corresponding evolution of the level sets. The simplest morphological smoothing model would be to consider mean curvature motion of the level sets (cf. Section II). But in addition to the smoothing of the level sets our aim is to maintain or even enhance edges on these surfaces. Edge type features on a smooth level set are characterized by a small curvature in the direction along the feature and a sufficiently large curvature in the perpendicular direction in the tangent space. For implicit surfaces these curvature quantities are represented by the shape operator $S = S(\phi) := D\,N$, where $N = \frac{\nabla\phi}{\|\nabla\phi\|}$. In the vicinity of an edge there will be a small and a large eigenvalue κ^1 and κ^2 respectively. The corresponding eigenvectors v^1 and v^2 point in tangential direction. The evaluation of the shape operator on a level set of a noisy image might be misleading with respect to the true but unknown level sets and edges. E. g. noise might be identified as features. Thus we have to consider a regularization in advance and prefilter the current image $\phi(t,\cdot)$ before evaluating the shape operator. We take into account a local L^2 projection of the image intensity on the space of quadratic polynomials. The width σ of the projection stencil is considered to be the parameter steering this regularization. The evaluation of the shape operator on this polynomials is straightforward. We end up with the following type of nonlinear parabolic problem. Given the initial 3D image ϕ_0 on a domain Ω, we ask for a scale of images $\{\phi(t,\cdot)\}_{t\geq 0}$ which obey the anisotropic

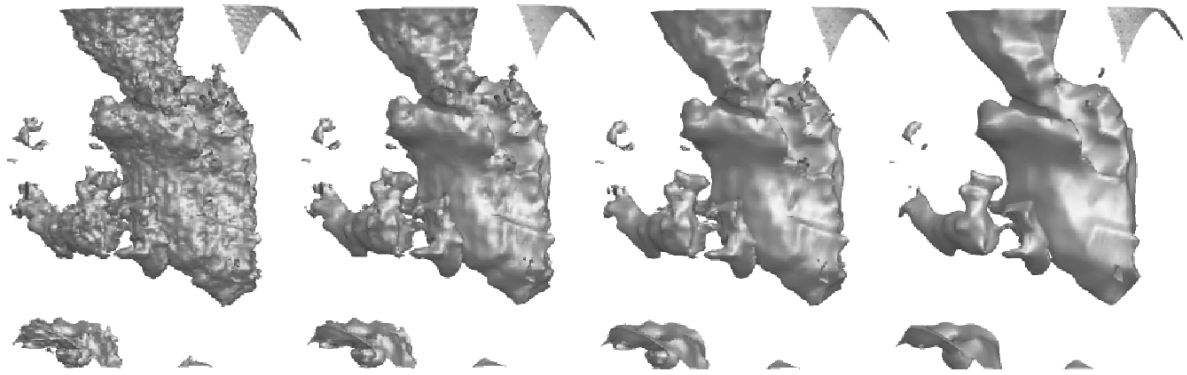

Fig. 2. *From left to right a certain level set - visualizing the shape of one ventricel of the human heart - is extracted from the anisotropic geometric evolution process for still images. Here successive steps of the smoothing process are shown. The computation was performed on a* 128^3 *grid.*

geometric evolution equation:

$$\partial_t \phi(t,x) - \|\nabla \phi(t,x)\| \operatorname{div}\left(a^\sigma(t,x)\,\frac{\nabla\phi}{\|\nabla\phi\|}(t,x)\right) = 0 \tag{1}$$

on $\mathbb{R}^+ \times \Omega$ and satisfy the initial condition

$$\phi(0,\cdot) = \phi_0(\cdot).$$

Furthermore, we suppose natural boundary conditions on $\partial\Omega$, i. e.

$$a^\sigma(t,x)\frac{\partial\phi}{\partial\nu}(t,x) = 0$$

where ν denotes the outer normal on $\partial\Omega$. The diffusion tensor a^σ is supposed to depend on the regularized shape operator S^σ

$$a^\sigma(t,x) := \mathcal{A}(S^\sigma(t,x))$$

where $\mathcal{A} : \mathrm{Sym}(\mathbb{R}^3) \to \mathrm{Sym}(\mathbb{R}^3)$. Here $\mathrm{Sym}(\cdot)$ denotes the space of symmetric maps. Finally $S^\sigma(x)$ is the shape operator at the position x evaluated on the local L^2 projection on quadratic polynomials with respect to a stencil ball $B_\sigma(x)$ of radius σ. As a suitable choice for this mapping $\mathcal{A}$ we consider the scalar function G from the basic image processing model, with $G(\alpha) = (1+\lambda^{-2}\alpha^2)^{-1}$, now acting on the shape operator of the projection. Mapping the normal space to the 0 we trivially expand it to $\mathrm{Sym}(\mathbb{R}^3)$. Here λ serves as a steering parameter for the identification of edges. The shape operator S^σ diagonalizes with respect to the basis $\{v^{1,\sigma}, v^{2,\sigma}, N^\sigma\}$, where $v^{1,\sigma}, v^{2,\sigma}$ are eigenvectors corresponding to principal curvatures $\kappa^{1,\sigma}, \kappa^{2,\sigma}$ on the level set and N^σ is the corresponding normal. Hence we obtain the matrix representation

$$\mathcal{A}(S^\sigma) = B_\sigma^T \begin{pmatrix} G(\kappa^{1,\sigma}) & & \\ & G(\kappa^{2,\sigma}) & \\ & & 0 \end{pmatrix} B_\sigma\,.$$

Here $B_\sigma \in SO(3)$ is the basis transformation from the regularized frame of principal directions of curvature and the normal $\{v^{1,\sigma}, v^{2,\sigma}, N^\sigma\}$ onto the canonical basis $\{e_1, e_2, e_3\}$.

In Figure 2 a 3D echocardiographical image of a human heart is taken as initial data. Here, different time steps of the evolution under anisotropic geometric diffusion are shown. A second example is concerned with true measurement data. The salt concentration in a density driven flow through a porous media filled with fresh and salt water is measured in a laboratory experiment by an MRI device. In Figure 3 level sets of the salt concentration are drawn, whereas Figure 4 shows slices through the 3D data set at different stages of the experiment. In both cases we compare the original measurement data with smoothing results obtained by our method.

Concerning the further details and an analysis of this model we refer to [26]. We especially observe that the underlying evolution is equivalent to the propagation of the level sets with speed f in normal direction N, i. e. $\partial_t x = f\,N$ holds for

$$f := \mathrm{tr}(\mathrm{a}^\sigma(\mathrm{S}_\sigma - \mathrm{S})) + (\operatorname{div}\mathrm{a}^\sigma)(\mathrm{N}^\sigma - \mathrm{N})\,.$$

Here we define $S_\sigma = DN^\sigma$, where N^σ is the normal of the locally projected image. This implies that our method is invariant on images ϕ_0 which are quadratic polyonomials.

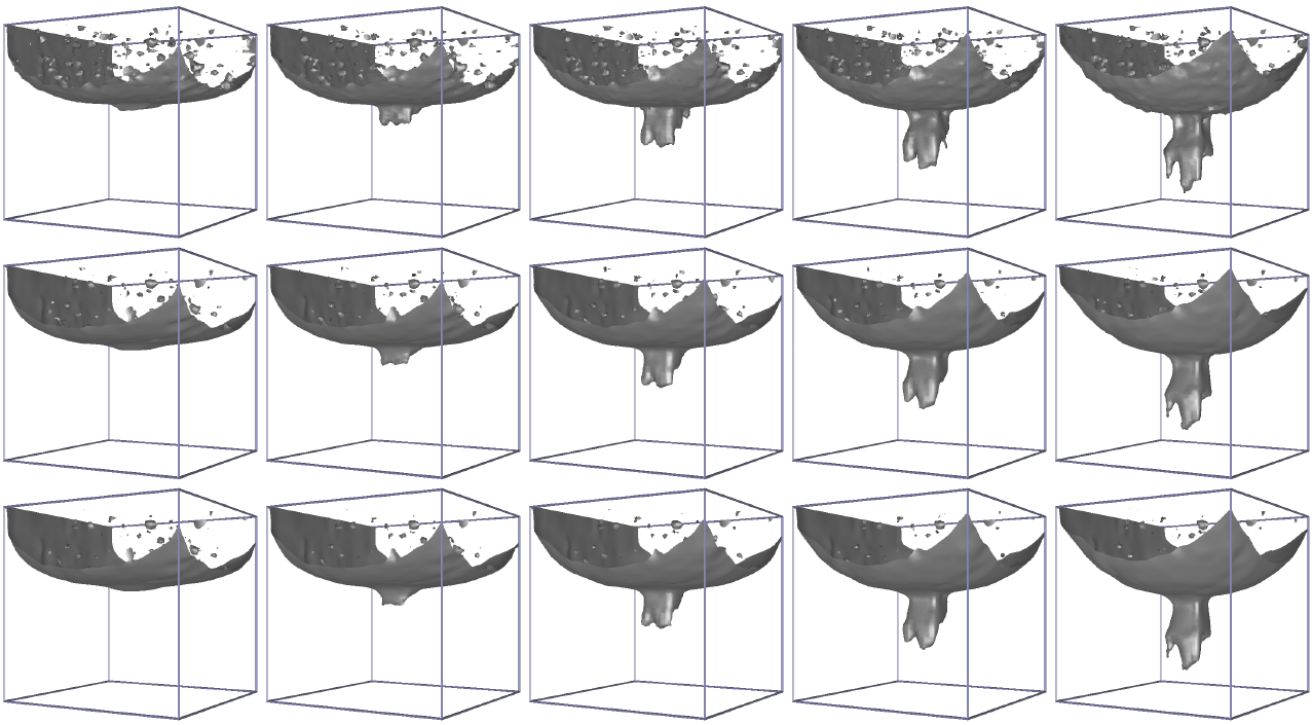

Fig. 3. *The anisotropic geometric level set method is applied to noisy data from a fingering experiment in a two phase porous medium flow of fresh and salt water. During the experiment the salt concentration was measured using an MR imaging device. From left to right different stages of the experiment (corresponding to different frames in the image sequence) are depcited. In the top row the original noisy data is shown, whereas in the second and third row the scale steps 2 respectively 3 of the coupled anisotropic evolution on a 64^3 grid are depicted (cf. also Fig. 4).*

IV. Processing image sequences via coupled anisotropic geometric diffusion

Let us now focus on the multiscale evolution of image sequences via an anisotropic geometric diffusion method. We therefore consider a grey valued image sequence $\phi_0 : [0,T]\times\Omega \to [0,1]$ where $[0,T]$ is the time interval of the given sequence. Our approach here is based on a combination of the ansitropic geometric diffusion method for still images (cf. Section III) applied to time slices of the sequence and a coupling of these initially seperate processes in the sequence parameter based on the approach presented in [14], [15], [29]. The coupling consists of the speed modulation via the clt-term which measures the curvature of a motion trajectory in the plane spanned by the normal on the level set of the image intensity and the apparent velocity [14], [15]. The curvature is proved to coincide with the acceleration of the normal component of the velocity in the direction of the apparent velocity. Thus, noisy motion trajectories will lead to a faster diffusion, which induces a smoothing. In Section VI we will outline that the proposed model is still handsome with respect the computation complexity also for large 3D image sequence. This holds true although we end up with a PDE in 5 dimensions: three spatial coordinates x , the sequence parameter s , and the scale parameter t .

I. e. we obtain the following problem:

For each frame $\phi_0(s,\cdot)$ of the image sequence find a scale of images $\{\phi(t,s,\cdot)\}_{t\geq 0}$ such that for $(t,s,x), \in \mathbb{R}^+ \times \{s\} \times \Omega$

$$\partial_t \phi(t,s,x) - \mathrm{clt}^\sigma(\phi)(t,s,x)\,\|\nabla\phi(t,s,x)\|\ \mathrm{div}\left(a^\sigma(t,s,x)\,\frac{\nabla\phi}{\|\nabla\phi\|}(t,s,x)\right) = 0$$

and in Ω

$$\phi(0,s,\cdot) = \phi_0(s,\cdot).$$

Furthermore, we suppose natural boundary conditions on $\partial\Omega$, i. e.

$$a^\sigma(t,s,x)\frac{\partial\phi}{\partial\nu}(t,s,x) = 0$$

where ν denotes the outer normal on $\partial\Omega$. Here, we take into account the same anisotropic diffusion tensor $a^\sigma(t,s,x)$ as in the case of still images, except the involved regularized shape operator $S^\sigma(t,s,x)$ is now evaluated for a time slice s in the image sequence $\phi(t,\cdot,\cdot)$. Furthermore, the curvature of lambertian trajectory $\mathrm{clt}(\phi)$ is evaluated on the spatially regularized image sequence. Indead we apply the same local projection of the image sequence time slices on quadratic polynomials and evaluate the operator $\mathrm{clt}(\cdot)$ for fixed position x and scale t on the family of resulting polynomials in s. Hence, the involved spatial regularization is indicated by an upper index σ.

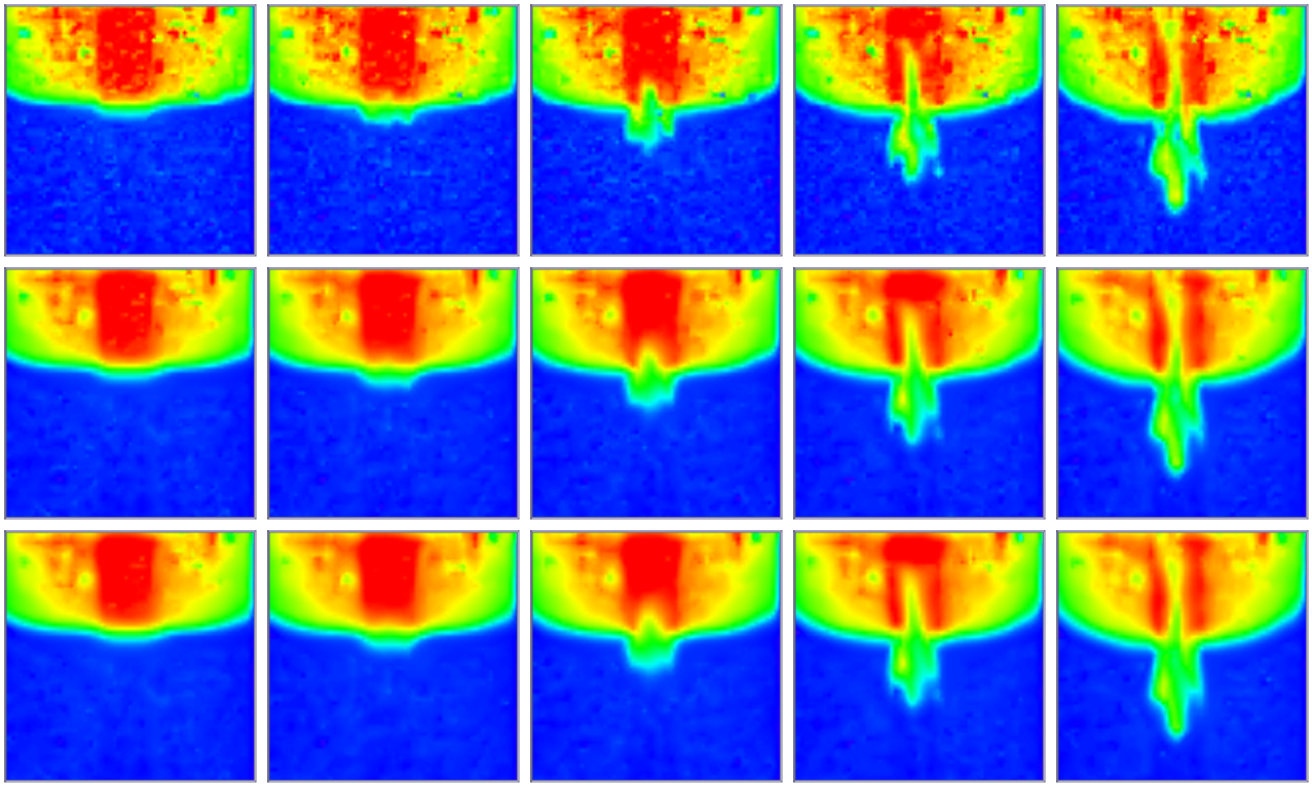

Fig. 4. *From the experimental data shown in Figure 3 vertical slices are extracted. Again from left to right different frames of the sequence and from top to bottom different scales from the evolution are shown.*

In general we can not guarantee that $\nabla\phi \neq 0$ and $\mathrm{clt}(\phi) \neq 0$ even if the initial data fulfills this regularity assumptions. Thus, we have to regularize the problem replacing the norm $\|\cdot\|$ in equation (1) and the $\mathrm{clt}(\cdot)$-term by a regular approximation. I. e. we choose

$$\begin{aligned} \|v\|_\epsilon &:= \sqrt{\epsilon^2 + \|v\|^2}\,, \\ \mathrm{clt}^\sigma(\psi)_\epsilon &:= \max\{\mathrm{clt}^\sigma(\psi), \epsilon\}\,. \end{aligned}$$

The corresponding regularized variational formulation is then given by ($\zeta = (t, s, x)$)

$$\left(\frac{\partial_t\phi(\zeta)}{\mathrm{clt}^\sigma(\phi)_\epsilon(\zeta)\,\|\nabla\phi(\zeta)\|_\epsilon}, \vartheta\right) + \left(a^\sigma(\zeta)\,\frac{\nabla\phi(\zeta)}{\|\nabla\phi(\zeta)\|_\epsilon}, \nabla\vartheta\right) = 0\,,$$

for all test functions $\vartheta \in C^\infty(\Omega)$. Here the brackets $(\cdot,\cdot)$ indicate the L^2 product on Ω. Considering a finite element implementation we will pick up this formulation in Section VI.

V. Local curvature and motion evaluation

In our model above we have made extensive use of a regularized shape operator S^σ and the curvature of lambertian trajectory term $\mathrm{clt}(\cdot)$, on which we base the computation of the anisotropic diffusion tensor and the speed modulation coupling the evolution problems on different time steps.

To this end let us fix a scale $t \in \mathbb{R}^+$. For each frame $\psi(s,\cdot) := \phi(t,s,\cdot)$ of the image sequence scale we consider a local L^2 projection in space of $\psi(s,\cdot)$ onto a subspace of the space of quadratic polynomials $\mathcal{P}_2$. Suppose we have fixed a point $x \in \Omega$ and we denote by $\mathcal{Q} := \mathrm{span}\{x_1^2, x_2^2, x_3^2,\, x_1x_2, x_1x_3, x_2x_3,\, x_1, x_2, x_3, 1\}$ this subspace of $\mathcal{P}_2$. The local L^2 projection $\Pi_{x,\sigma}\psi(s,\cdot) \in \mathcal{Q}$ of the intensity $\psi(s,\cdot)$ onto $\mathcal{Q}$ is then defined via the orthogonality relation

$$\int_{\mathcal{B}_\sigma(x)} (\psi(s, y-x) - (\Pi_{x,\sigma}\psi)(s,y))\; q\; dy = 0 \qquad \forall\, q \in \mathcal{Q},$$

where $\mathcal{B}_\sigma(x)$ is a ball of radius σ around x. For the ease of presentation we write $\psi^\sigma_{s,x}(y)$ instead of $(\Pi_{s,x,\sigma}\psi)(y)$ for fixed $(s,x) \in [0,T] \times \Omega$ in case of the local L^2 projection applied to an image frame. Now we define in analogy to the non-regularized

case the shape operator $S^\sigma(s,x) = S(\psi^\sigma_{s,x}(\cdot))(x) := (D_y N^\sigma)(x)$ (cf. Section III), with $N^\sigma(y) = \frac{\nabla_y \Psi^\sigma_{s,x}(y)}{\|\nabla_y \Psi^\sigma_{s,x}(y)\|}$. Thus, S^σ is charaterized by its eigenvalues 0, $\kappa^{j,\sigma}$, $j = 1,2$ and the eigenvectors $\{v^{1,\sigma}, v^{2,\sigma}, N^\sigma\}$. Therefore, with an appropriate basis transformation $B_\sigma \in SO(3)$, we obtain

$$S^\sigma = B_\sigma^T \begin{pmatrix} \kappa^{1,\sigma} & & \\ & \kappa^{2,\sigma} & \\ & & 0 \end{pmatrix} B_\sigma .$$

Furthermore we will base the evaluation of the curvature of the lambertian trajectory on the locally projected images. Hence, in anticipation of a later discrete sequence of frames we consider the local projections of a previous ($s - \Delta s$), the actual (s) and a next frame ($s + \Delta s$), respectively. Then we compute the clt-term by the following formula

$$\begin{aligned} \mathrm{clt}^\sigma(\psi)(t,s,x) := \min_{w_1,w_2 \in B_\sigma(x)} \frac{1}{(\Delta s)^2} \Big(& \langle \nabla \psi^\sigma_{s,x}(0), w_1 - w_2 \rangle \\ & + |\psi^\sigma_{s-\Delta s,x}(w_1) - \psi^\sigma_{s,x}(0)| \\ & + |\psi^\sigma_{s+\Delta s,x}(w_2) - \psi^\sigma_{s,x}(0)| \Big), \end{aligned}$$

since we have shifted the projections locally such that $\psi^\sigma_{s,x}(0) = \phi(t,s,x)$. The evaluation of the clt-term can be done via testing a lattice of different $w_i \in B_\sigma(x)$ or by a continous minimization of the resulting polynomial. In our implementation we currently apply the lattice approach.

VI. Finite element discretization

Up to now we have considered an image intensity $\phi(t,s,x)$ which has been a sufficiently smooth function on $R^+ \times [0,T] \times \Omega \subset \mathbb{R}^3$. Concerning the implementation of the proposed multiscale method and its actual application to digital image sequences we now have to discretize our model in space and in the scale parameter t. First, as already mentioned we consider our image sequence to consist of $m+1$ frames at time steps $\Delta s := \frac{T}{m}$. In applications these image frames typically arise as arrays of pixels. We interprete pixel values as nodal values on a uniform hexahedral mesh $\mathcal{C}$ covering the whole image domain Ω and consider the corresponding trilinear interpolation on cells $C \in \mathcal{C}$ to obtain discrete intensity functions in the accompanying finite element space. To clarify the notation we will always denote spatially discrete quantities with upper case letters to distinguish them from the corresponding continuous quantities in lower case letters. A sub- or superscript h indicates the grid size, an upper index the time step, and a lower index the processed frame, i.e. $\Phi_i(t,x) = \Phi(t, i\Delta s, x)$. Let us define the space of piecewise trilinear, continuous functions

$$V^h = \{ \Phi \in C^0(\Omega) \mid \Phi|_C \in \mathcal{P}_1 \otimes \mathcal{P}_1 \otimes \mathcal{P}_1 \, \forall C \in \mathcal{C} \} ,$$

where $\mathcal{P}_1$ denotes the space of linear polynomials and $\otimes$ the tensor product. Discretizing first only in space we obtain a variational finite element formulation of our level set evolution problem:

For $i = 0, \ldots, m$ find $\Phi_i : \mathbb{R}_0^+ \to V^h$ with initial data $\Phi_i(0) = \mathcal{I}_h \phi_0(i\Delta s)$, such that

$$\left(\frac{\partial_t \Phi_i}{\mathrm{clt}^\sigma(\Phi)_\epsilon \, \|\nabla \Phi_i\|_\epsilon}, \theta \right)^h + \tau \left(A_i^\sigma \frac{\nabla \Phi_i}{\|\nabla \Phi_i\|_\epsilon}, \nabla \theta \right) = 0$$

for all $\theta \in V^h$.

Here, $\mathcal{I}_h : C^0(\Omega) \to V^h$ is the Lagrange interpolation on the grid $\mathcal{C}$ and the diffusion tensor A_i^σ is supposed to be a suitable approximation of $a^\sigma(t, i\Delta s, \cdot)$. Finally, we have used the lumped mass scalar product $(\cdot,\cdot)^h$, which is defined by

$$(U,V)^h := \sum_{C \in \mathcal{C}} \int_C \mathcal{I}_h(U\,V) \, \mathrm{d}x$$

for discrete functions $U, W \in V^h$ (cf. [33]). As an immediate consequence the corresponding nonlinear mass matrix $M_h(\Phi)$ is diagonal. This simplifies the resulting scheme significantly. We end up with a system of ordinary differential equations for the nodal values of the intensity function Φ. Following Dziuk and Deckelnick [10] we select $\epsilon \approx h$. Furthermore we consider a stencil width $\sigma = C\,h$ for integers C equal to $2, 3$ or 4.

Next, we have to discretize in time, which includes the choice of some time stepping scheme and the decision which term to be handled implicitly and which explicitly. Here we choose a semi-implicit backward Euler discretization. Expressed in geometric terms we consider the metric and the regularized shape operator explicitly for each frame(cf. [12]). Let τ be a selected scale step size and let Φ_i^n to be an approximation of $\Phi_i(n\tau)$. Then we obtain the time and space discrete problem:

For $i = 0, \ldots, m$ find a sequence of discrete intensity functions $\{\Phi_i^n\}_{n=0,\cdots}$ with $\Phi_i^n \in V^h$ and $\Phi_i^0 = \mathcal{I}_h \phi_0(i\Delta s)$, such that

$$\left(\frac{\Phi_i^{n+1} - \Phi_i^n}{\mathrm{clt}^\sigma(\Phi^n)_\epsilon \, \|\nabla \Phi_i^n\|_\epsilon}, \theta \right)^h + \tau \left(A_i^{\sigma,n} \frac{\nabla \Phi_i^{n+1}}{\|\nabla \Phi_i^n\|_\epsilon}, \nabla \theta \right) = 0$$

for all $\theta \in V^h$.

Finally, in each step of the discrete evolution, for each frame in the image sequence we have to solve a single system of linear equations. In terms of nodal vectors indicated by a bar on top of the corresponding discrete function we can rewrite the scheme and get

$$\left(M_h(\Phi_i^n) + \tau L_h(\Phi_i^n)\right) \bar{\Phi}_i^{n+1} = M_h(\Phi_i^n) \bar{\Phi}_i^n$$

for the new vector of nodal values $\bar{\Phi}_i^{n+1}$ at time $t_{n+1} = (n+1)\tau$. Here, we have applied the nonlinear lumped mass and stiffness matrices

$$M_h(\Phi_i^n) = \left(\left(\frac{\Psi_\mu}{\mathrm{clt}^\sigma(\Phi^n)_\epsilon \, \|\nabla \Phi_i^n\|}, \Psi_\nu \right)^h \right)_{\mu\nu},$$

$$L_h(\Phi_i^n) = \left(\left(A_i^{n,\sigma} \frac{\nabla \Psi_\mu}{\|\nabla \Phi_i^n\|_\epsilon}, \nabla \Psi_\nu \right) \right)_{\mu\nu},$$

where $\{\Psi_\mu\}_\mu$ is the nodal basis of V^h.

In each time step the discrete diffusion tensor $A_i^{n,\sigma}$ and $\mathrm{clt}(\Phi^n)_\epsilon$ are evaluated for every grid node and every image frame separately. Then, on cells $C \in \mathcal{C}$ we use trilinear interpolation to define $A_i^{n,\sigma}$. Furthermore, in the numerical application we have replaced the integration of $(A_i^{n,\sigma} \frac{\nabla \Psi_\mu}{\|\nabla \Phi_i^n\|_\epsilon}, \Psi_\nu)$ by the one point numerical quadrature which refers only to the value at the element's center of mass.

Concerning the proper choice of the stencil parameter σ with respect to the grid size we refer to [26].

ACKNOWLEDGEMENTS

The echocardiographical data show in Figure 2 was provided by TomTec Imaging Systems and C. Lamberti from DEIS, Bologna University. Furthermore we acknowledge Sascha Oswald from Sheffield University, who performed the fresh and salt water experiment shown in Figures 3 and 4.

REFERENCES

[1] L. Alvarez, F. Guichard, P. L. Lions, and J. M. Morel. Axioms and fundamental equations of image processing. *Arch. Ration. Mech. Anal.*, 123(3):199–257, 1993.

[2] L. Alvarez, J. Weickert, and J. Sánchez. A scale–space approach to nonlocal optival flow calculations. In M. Nielsen, P. Johansen, O. F. Olsen, and J. Weickert, editors, *Scale-Space Theories in Computer Vision. Second International Conference, Scale-Space 1999, Corfu, Greece, September 1999*, Lecture Notes in Computer Science; 1682, pages 235–246. Springer, 1999.

[3] S. B. Angenent and M. E. Gurtin. Multiphase thermomechanics with interfacial structure 2, evolution of an is othermal interface. *Arch. Rational Mech. Anal.*, 108:323–391, 1989.

[4] E. Bänsch and K. Mikula. A coarsening finite element strategy in image selective smoothing. *Computing and Visualization in Science*, 1:53–63, 1997.

[5] G. Bellettini and M. Paolini. Anisotropic motion by mean curvature in the context of finsler geometry. *Hokkaido Math. J.*, 25:537–566, 1996.

[6] F. Catté, P.-L. Lions, J.-M. Morel, and T. Coll. Image selective smoothing and edge detection by nonlinear diffusion. *SIAM J. Numer. Anal.*, 29(1):182–193, 1992.

[7] U. Clarenz, U. Diewald, and M. Rumpf. Nonlinear anisotropic diffusion in surface processing. In *Proc. Visualization 2000*, pages 397–405, 2000.

[8] C. A. Davatzikos, R. N. Bryan, and J. L. Prince. Image registration based on boundary mapping. *IEEE Trans. Medical Imaging*, 15(1):112–115, 1996.

[9] K. Deckelnick and G. Dziuk. Discrete anisotropic curvature flow of graphs. *Mathematical Modelling and Numerical Analysis, to appear*, 2000.

[10] K. Deckelnick and G. Dziuk. A fully discrete numerical scheme for weighted mean curvature flow. Technical Report 30, Mathematische Fakultät Freiburg, 2000.

[11] R. Deriche, P. Kornprobst, and G. Aubert. Optical–flow estimation while preserving its discontinuities: A variational approach. In *Proc. Second Asian Conf. Computer Vision (ACCV '95, Singapore, December 5–8, 1995)*, volume 2, pages 290–295, 1995.

[12] G. Dziuk. An algorithm for evolutionary surfaces. *Numer. Math.*, 58:603–611, 1991.

[13] L. Evans and J. Spruck. Motion of level sets by mean curvature I. *J. Diff. Geom.*, 33(3):635–681, 1991.

[14] F. Guichard. *Axiomatisation des analyses multi-échelles d́images et de films*. PhD thesis, University Paris IX Dauphine, 1994.

[15] F. Guichard. A morphological, affine, and galilean invariant scale–space for movies. *IEEE Transactions on Image Processing*, 7(3):444–456, 1998.

[16] J. Kačur and K. Mikula. Solution of nonlinear diffusion appearing in image smoothing and edge detection. *Appl. Numer. Math.*, 17 (1):47–59, 1995.

[17] R. Kimmel. Intrinsic scale space for images on surfaces: The geodesic curvature flow. *Graphical Models and Image Processing*, 59(5):365–372, 1997.

[18] F. Maes, A. Collignon, D. Vandermeulen, G. Marchal, and P. Suetens. Multi–modal volume registration by maximization of mutual information. *IEEE Trans. Medical Imaging*, 16(7):187–198, 1997.

[19] K. Mikula and J. Kačur. Evolution of convex plane curves describing anisotropic motions of phase interfaces. *SIAM Journal on Scientific Computing*, 17(6):1302–1327, 1996.

[20] K. Mikula and N. Ramarosy. Semi–implicit finite volume scheme for solving nonlinear diffusion equations in image processing. *Numerische Mathematik*, 2001.

[21] K. Mikula, A. Sarti, F. Sgallari, and C. Lamberti. *Nonlinear multiscale analysis models for filtering of 3D + time biomedical images*. Lectures Notes in Computational Science and Eng. Springer Verlag, 2001.

[22] H. H. Nagel and W. Enkelmann. An investigation of smoothness constraints for the estimation of displacement vector fields from images sequences. *IEEE Trans. Pattern Anal. Mach. Intell.*, 8:565–593, 1986.

[23] E. Pauwels, P. Fiddelaers, and L. Van Gool. Enhancement of planar shape through optimization of functionals for curves. *IEEE Trans. Pattern Anal. Mach. Intell.*, 17:1101–1105, 1995.
[24] P. Perona and J. Malik. Scale space and edge detection using anisotropic diffusion. In *IEEE Computer Society Workshop on Computer Vision*, 1987.
[25] T. Preußer and M. Rumpf. An adaptive finite element method for large scale image processing. *Journal of Visual Comm. and Image Repres.*, 11:183–195, 2000.
[26] T. Preußer and M. Rumpf. A level set method for anisotropic diffusion in 3D image processing. *SIAM J. Appl. Math.*, 2001, to appear.
[27] E. Radmoser, O. Scherzer, and J. Weickert. Scale–space properties of regularization methods. In M. Nielsen, P. Johansen, O. F. Olsen, and J. Weickert, editors, *Scale-Space Theories in Computer Vision. Second International Conference, Scale-Space '99, Corfu, Greece, September 1999*, Lecture Notes in Computer Science; 1682, pages 211–220. Springer, 1999.
[28] G. Sapiro. Vector (self) snakes: A geometric framework for color, texture, and multiscale image segmentation. In *Proc. IEEE International Conference on Image Processing, Lausanne*, September 1996.
[29] A. Sarti, K. Mikula, and F. Sgallari. Nonlinear multiscale analysis of 3D echocardiography sequences. *IEEE Transactions of Medical Imaging*, 18(6):453–466, 1999.
[30] C. Schnoerr. A study of a convex variational diffusion approach for image segmentation and feature extraction. *J. Math. Imaging Vis.*, 8(3):271–292, 1998.
[31] J. E. Taylor, J. W. Cahn, and C. A. Handwerker. Geometric models of crystal growth. *Acta metall. mater.*, 40:1443–1474, 1992.
[32] J. P. Thirion. Image matching as a diffusion process: An analogy with maxwell's demon. *Medical Imag. Analysis 2*, pages 243–260, 1998.
[33] V. Thomee. *Galerkin - Finite Element Methods for Parabolic Problems.* Springer, 1984.
[34] J. Weickert. *Anisotropic diffusion in image processing.* Teubner, 1998.